Research article

BDNF-induced BDNF release mediates presynaptic LTP and is regulated by cannabinoids

Coralie Berthoux[1], Kaoutsar Nasrallah[1] and Pablo E. Castillo[1,2]*

[1]Dominick P. Purpura Department of Neuroscience, Albert Einstein College of Medicine, Bronx, United States
[2]Department of Psychiatry and Behavioral Sciences, Albert Einstein College of Medicine, Bronx, United States

Running title: BDNF-induced BDNF release

Keywords: Dentate gyrus, hippocampus, cannabinoids, enriched environment

*To whom correspondence should be addressed:
Pablo E. Castillo, MD/PhD
Dominick P. Purpura Department of Neuroscience
Albert Einstein College of Medicine
1410 Pelham Parkway South
Kennedy Center, Room 703
Bronx, NY 10461, USA
Email: pablo.castillo@einsteinmed.org

Title: 83 characters (with spaces)
Total number of words
Summary: 150; Introduction: 795; Results: 2170;
Discussion: 1646; Methods: 1538
Total character count in this entire document (excluding Methods): 44697
Figures: 7
Supplemental Figures: 4
Supplemental Table: 1
The authors declare no competing financial interests.

Abstract

Although brain-derived neurotrophic factor (BDNF) and its effector, Tropomyosin receptor kinase B (TrkB), are implicated in activity-dependent synaptic plasticity, the precise underlying mechanisms remain unclear. In the dentate gyrus, a hippocampal input region that expresses uniquely high levels of BDNF, repetitive activation of mossy cells (MCs) induces a presynaptic, BDNF/TrkB-dependent form of LTP at MC to granule cell (GC) synapses. Here, we report that activity-induced BDNF release from MC axons in mice elicits postsynaptic BDNF release in a TrkB- and calcium-dependent manner, and that BDNF-induced BDNF release is essential for LTP induction. Suppression of BDNF release by tonic and phasic activity of presynaptic type-1 cannabinoid receptors dampened LTP, revealing an unprecedented role of these receptors in controlling neuropeptide release. Lastly, BDNF-mediated MC-GC LTP can be elicited *in vivo*. Thus, BDNF-induced BDNF release emerges as a mechanism for activity-dependent LTP that may contribute to dentate gyrus-dependent learning, epilepsy, and neuropsychiatric disorders.

Highlights:

- Pre- and postsynaptic BDNF are both required for presynaptic LTP in the dentate gyrus
- BDNF is released from MC axons and GC proximal dendrites following repetitive activation of MC axons
- Presynaptic BDNF release is inhibited by activation of CB_1R expressed on MC axons
- BDNF is sufficient to trigger postsynaptic BDNF release from GCs in a TrkB- and calcium-dependent manner
- Enriched environment induces BDNF-dependent LTP of MC-GC synapses *in vivo*

In Brief:

Berthoux et al. describe a novel mechanism of presynaptic LTP that requires BDNF-induced BDNF release. This BDNF-mediated plasticity can occur *in vivo* and is tightly controlled by cannabinoid activity.

INTRODUCTION

The mechanisms underlying experience-dependent synaptic plasticity, such as long-term potentiation (LTP), are remarkably diverse and remain not fully understood (Citri and Malenka, 2008; Monday et al., 2018). Among these mechanisms, the brain-derived neurotrophic factor (BDNF) has been proposed as a key regulator of synaptic efficacy, neural connectivity, and experience-dependent plasticity (Edelmann et al., 2014; Lu et al., 2014; Park and Poo, 2013; Sasi et al., 2017). Consistent with these roles, BDNF is implicated in neural development, learning and memory (Korte et al., 1998; Minichiello, 2009; Minichiello et al., 1999; Park and Poo, 2013). BDNF is a soluble peptide and, in the adult brain, signals mainly through the Tropomyosin receptor kinase B (TrkB) located at pre- and/or postsynaptic sites (Minichiello, 2009; Park and Poo, 2013). BDNF is stored in dense core vesicles and released upon activity in a calcium- and SNARE-dependent manner (Dieni et al., 2012; Shimojo et al., 2015). However, how exactly BDNF/TrkB signaling mediates synaptic plasticity remains unclear. Several key questions remain unanswered, including the kind of activity required to release BDNF and induce experience-dependent synaptic plasticity, the pre- and/or postsynaptic source of BDNF, and whether and how BDNF release is regulated (Brigadski and Lessmann, 2020; Edelmann et al., 2014).

The dentate gyrus (DG), a key entry area of the hippocampus, expresses uniquely high levels of BDNF (Conner et al., 1997; Dieni et al., 2012; Yan et al., 1997b). Within the DG, two excitatory neurons, dentate granule cells (GCs) and hilar mossy cells (MCs), are reciprocally connected, thereby establishing a recurrent excitatory circuit (Amaral et al., 2007). GCs send their axons to the proximal dendrites of MCs, and MCs send their axons to the inner molecular layer (IML) to excite the proximal dendrites of GCs (Buckmaster and Soltesz, 1996; Scharfman, 2016). This associative GC→MC→GC circuit is believed to play key roles in DG-dependent learning (e.g., pattern-separation) (Jinde et al., 2012; Kesner and Rolls, 2015; Rolls, 2013), and dysregulation of this circuit is implicated in epilepsy (Scharfman, 2016). Remarkably, BDNF expression is particularly high in the IML (Conner et al., 1997; Dieni et al., 2012; Yan et al., 1997b), and TrkB are strongly expressed in both GC layer (GCL) and IML (Donovan et al., 2008; Drake et al., 1999; Yan et al., 1997a). Repetitive activation of MC axons induces a robust LTP at MC-GC synapses (MC-GC LTP) that requires postsynaptic BDNF/TrkB signaling and is presynaptically expressed as a long-lasting increase in glutamate release (Hashimotodani et al., 2017). Unlike most forms of LTP at glutamatergic synapses, induction of MC-GC LTP does not require NMDA receptor activation or activation of any other ionotropic or metabotropic glutamate receptor (Hashimotodani

et al., 2017; Jensen et al., 2021), suggesting that the release of BDNF, rather than glutamate, triggers MC-GC LTP.

BDNF release is a highly regulated process (Brigadski and Lessmann, 2020). The key role of BDNF at strengthening MC-GC synapses under normal and pathological conditions (Hashimotodani et al., 2017; Nasrallah et al., 2021b) strongly suggests that some mechanism controls its release from MC axon boutons. Endocannabinoids (eCBs) are excellent candidates given that these retrograde signals are typically released upon activity to robustly suppress neurotransmitter release by activating type-1 cannabinoid receptors (CB_1Rs) (Castillo et al., 2012). Remarkably, MC axon terminals express uniquely high levels of CB_1Rs (Katona et al., 2006; Monory et al., 2006; Uchigashima et al., 2011), whose activation suppresses glutamate release (Chiu and Castillo, 2008). Moreover, recent evidence indicates that tonic (constitutively active, ligand-*in*dependent) and phasic (ligand-dependent) CB_1R activity inhibits MC-GC synaptic transmission and plasticity (Jensen et al., 2021). While the effect on synaptic transmission relies on the inhibition of voltage-gated calcium channels (VGCCs) and the cAMP/PKA cascade, the underlying mechanism implicated in LTP dampening is unclear. There is strong evidence that BDNF can control synaptic function by regulating eCB signaling (Gangarossa et al., 2020; Lemtiri-Chlieh and Levine, 2010; Wu et al., 2020). However, whether and how eCB signaling controls BDNF release is unknown.

In the present study, we characterized BDNF release and its regulation at MC-GC synapses using electrophysiology and optogenetics in mouse acute hippocampal slices, direct measurement of activity-induced BDNF secretion using 2-photon imaging, and a cell-type selective conditional knock-out (cKO) approach. We report that BDNF is released from the pre- and postsynaptic compartments upon MC burst activity, and that presynaptic BDNF triggered postsynaptic BDNF release via TrkB activation and mobilization of postsynaptic calcium internal stores. BDNF-induced BDNF release was critical for the induction of MC-GC LTP. Moreover, CB_1Rs dampen MC-GC LTP by suppressing presynaptic BDNF release in a tonic and phasic manner. Finally, we provide evidence that BDNF-dependent MC-GC LTP occurs *in vivo* and may contribute to DG-dependent forms of learning and memory. Altogether, our findings uncover novel mechanisms of presynaptic plasticity involving BDNF/TrkB signaling and CB_1R-mediated regulation of BDNF release at a key hippocampal circuit.

RESULTS

Presynaptic BDNF release is required for MC-GC LTP

MC-GC LTP requires postsynaptic BDNF/TrkB signaling (Hashimotodani et al., 2017), and BDNF is densely expressed in the IML (Conner et al., 1997). However, the source of BDNF release is unclear. Given that bursts of MC activity trigger this form of plasticity, we first examined whether BDNF released from MC axons is required for induction. To directly test this possibility, we selectively and conditionally removed *Bdnf* from MCs. Taking advantage of the MC commissural projections, we injected a mix of Cre recombinase-containing AAV (AAV5.CamKII.mCherry-Cre) and Cre-dependent ChiEF (1:2 ratio) into one DG of *Bdnf*$^{fl/fl}$ (Pre *Bdnf* cKO) or WT (control) mice and analyzed the contralateral DG. This approach allowed us to optically activate Cre-positive (i.e., Pre *Bdnf* cKO in *Bdnf*$^{fl/fl}$ mice) MC axon terminals in the IML (Fig. 1A–B). Paired-pulse ratio (PPR) and coefficient of variation (CV) were unchanged, indicating that presynaptic *Bdnf* deletion did not affect basal MC-GC presynaptic function (Fig. 1C). However, MC-GC LTP was abolished in Pre *Bdnf* cKO mice as compared to controls (Fig. 1D). In contrast, and in agreement with the fact that presynaptic PKA activation downstream BDNF/TrkB signaling is necessary and sufficient for MC-GC LTP (Hashimotodani et al., 2017), bath application of the adenylyl cyclase activator forskolin (50 μM for 10 min) was still able to potentiate MC-GC synaptic transmission in Pre *Bdnf* cKO mice similar to controls (Fig. 1E). Together, these findings strongly suggest that the lack of MC-GC LTP was due to the absence of presynaptic BDNF in MC terminals.

To directly visualize and characterize activity-dependent BDNF release from MC axons, we utilized a BDNF reporter (BDNF-pHluorin or BDNF-pH) (Matsuda et al., 2009; Park, 2018; Park et al., 2014). To restrict the expression of BDNF-pH in MC axon terminals, a mix of Cre recombinase-containing AAV (AAV5.CamKII.mCherry-Cre) and Cre-dependent BDNF-pH (1:2 ratio) was injected into one DG of WT mice (Fig. 1F). Four weeks post-injection, we observed a high-level BDNF-pH expression in commissural MC axons of the contralateral IML (Fig. 1G–H). To assess activity-dependent BDNF release, we monitored changes in the fluorescence intensity of BDNF-pH puncta (1–3 μm), which represent BDNF-containing presynaptic boutons, using time-lapsed 2-photon microscopy of acute hippocampal slices (Fig. 1H). We found that repetitive activation of MC axons (MC bursts) using the same protocol that induces MC-GC LTP (5 pulses, 100 Hz, repeated 50 times every 0.5 s) significantly reduced BDNF-pH fluorescence intensity (Fig. 1I and 1K–L). Consistent with the requirement for calcium influx via VGCCs to release BDNF (Brigadski and Lessmann, 2020; Matsuda et al., 2009), the reduction in BDNF-pH fluorescence

was abolished by adding the non-selective VGCC blocker cadmium (100 μM) to the recording solution (Fig. 1J–L). These results indicate that repetitive activation of MC axons that induces MC-GC LTP, releases BDNF from axon terminals in a presynaptic calcium influx-dependent manner.

CB_1R activity negatively regulates presynaptic BDNF secretion from MC axon terminals

MC axon boutons express high levels of CB_1Rs (Katona et al., 2006; Monory et al., 2006; Uchigashima et al., 2011), which inhibit glutamate release and MC-GC LTP induction in a tonic (constitutively active, ligand-independent) and phasic (ligand-dependent) manner (Jensen et al., 2021). Given that LTP induction is completely independent of glutamate transmission (Jensen et al., 2021), while it requires BDNF/TrkB signaling, we tested whether presynaptic CB_1Rs could dampen LTP by suppressing BDNF release from MC axonal boutons. To this end, we pre-incubated acute hippocampal slices with the CB_1R agonist WIN 55,212-2 (5 μM for 25 min), which was also perfused in the recording chamber, and found that WIN blocked BDNF release following the MC-GC LTP induction protocol (Fig. 2A and 2C–D), whereas this effect was prevented by a CB_1R inverse agonist AM251 (5 μM) (Fig. 2B–D). These results indicate that activation of CB_1R negatively regulates BDNF release from MC axons. In addition to this ligand-dependent effect via presynaptic CB_1R activation, presynaptic BDNF release could also be under the control of tonic CB_1R activity. To test this possibility, MC axons were stimulated with bursts known to induce a submaximal LTP (e.g., 30 Hz instead of 100 Hz burst used in Fig. 1F–L) which is facilitated when blocking CB_1R constitutive activity with the inverse CB_1R agonist AM251 (Jensen et al., 2021). If this facilitation is due to the blockade of CB_1R tonic activity, AM251 should also increase BDNF release. We found that blocking tonic CB_1R activity with 5 μM AM251 facilitated presynaptic BDNF release, as indicated by a large reduction in BDNF-pH fluorescence intensity when blocking CB_1R activity as compared to controls (Fig. 2F and 2G–H). The fact that submaximal LTP induction protocol was not associated with any significant change in fluorescence in absence of AM251 (Fig. 2E and 2G–H) is likely due to a poor sensitivity of BDNF-pHluorin. These results indicate that CB_1R activity inhibits presynaptic BDNF release and negatively regulates MC-GC LTP induction, underscoring a novel role of CB_1R in regulating neuropeptide release.

Postsynaptic BDNF is also required for MC-GC LTP induction

BDNF is found in GC dendrites (Conner et al., 1997) from where it could be released to activate postsynaptic TrkB in an autocrine manner (Harward et al., 2016), or target presynaptic TrkB in a

retrograde manner (Jakawich et al., 2010; Lin et al., 2018). To test whether postsynaptic BDNF is also involved in MC-GC LTP, we conditionally and selectively knock out *Bdnf* from GCs by injecting AAV5.CamKII.mCherry-Cre (Post *Bdnf* cKO) or AAV5.CamKII.mCherry (control) in the upper GCL of *Bdnf*$^{fl/fl}$ mice (Fig. 3A) and recorded MC-elicited EPSCs from mCherry-positive GCs (Fig. 3B). Deleting *Bdnf* from GCs had no significant effect on basal MC-GC PPR and CV (Fig. 3C). Surprisingly, MC-GC LTP was abolished in Post *Bdnf* cKO (Fig. 3D), while forskolin-induced LTP was unaffected (Fig. 3E), consistent with cAMP/PKA acting downstream of BDNF/TrkB signaling (Hashimotodani et al., 2017).

These results suggest that burst stimulation of MC axons releases BDNF from GCs, which is required for the induction of MC-GC LTP. To directly test this possibility, we measured postsynaptic BDNF release selectively, by expressing BDNF-pH in the upper GCL of WT mice (Fig. 4A). At 10 days post-injection, we observed high-level of BDNF-pH in the soma and proximal dendrites of GCs, but not in MCs of the ipsilateral DG (Fig. 4B–C). MC burst stimulation significantly reduced BDNF-pH fluorescence intensity from GC proximal dendrites (Fig. 4D and 4F–G). Although BDNF release could result from postsynaptic firing (Brigadski and Lessmann, 2020), we previously found that MC bursts are not sufficient to induce GC firing under our experimental conditions (i.e. in absence of GABA receptor antagonists) (Hashimotodani et al., 2017). Lastly, postsynaptic BDNF release was abolished by the TrkB antagonist ANA-12 (15 μM for 25 min) (Fig. 4E and 4F–G), suggesting that postsynaptic BDNF release requires TrkB activation. Altogether, our findings indicate that presynaptic burst activity triggers postsynaptic BDNF release in a TrkB-dependent manner, and that release of postsynaptic BDNF is required for the induction of LTP at MC-GC synapses.

Postsynaptic, but not presynaptic, activation of TrkB is necessary for BDNF release and MC-GC LTP

Given that activation of postsynaptic TrkB is necessary to induce MC-GC LTP (Hashimotodani et al., 2017), we directly measured BDNF release from GC lacking TrkB (Post *TrkB* cKO) by injecting AAV5.CamKII.mCherry-Cre alongside with Cre-dependent BDNF-pH into the DG of *TrkB*$^{fl/fl}$ mice or WT (control) littermates. We found that burst stimulation of MC axons significantly reduced BDNF-pH fluorescence intensity in controls (Fig. 4H and 4J–K), but not in Post *TrkB* cKO mice (Fig. 4G and 4J–K), suggesting that presynaptically released BDNF, by activating postsynaptic TrkB, promotes BDNF release from GCs.

BDNF could also activate presynaptic TrkB (Inagaki et al., 2008; Jakawich et al., 2010; Lin et al., 2018; Liu et al., 2007), thereby facilitating further BDNF release from MC axons. To test this possibility, we selectively and conditionally removed *TrkB* from MC axon terminals by injecting a mix of AAV5.CamKII.mCherry-Cre and Cre-dependent ChiEF (1:2 ratio) into the DG of *TrkB*$^{fl/fl}$ (Pre *TrkB* cKO) or WT (control) littermates. This approach allowed us to optically activate Cre-positive (i.e., Pre *TrkB* cKO in *TrkB*$^{fl/fl}$ mice mice) MC axon terminals in the IML of the contralateral hippocampus (Fig. S1A–B). We found that MC-GC LTP was normally induced in Pre *TrkB* cKO mice as compared to controls (Fig. S1C), suggesting that presynaptic TrkB expressed on MC axons are not implicated in MC-GC LTP induction.

BDNF is sufficient to induce BDNF release from GC proximal dendrites

Thus far, our results strongly suggest that BDNF is required to induce BDNF release from GCs. To test whether BDNF is also sufficient for postsynaptic BDNF secretion, we monitored BDNF-pH fluorescence intensity and applied a human recombinant BDNF (8 nM for 10 min) in the recording chamber. We found that exogenous BDNF application induced BDNF release from GCs (Fig. 5A and 5D–E), and this effect was abolished in the presence of the TrkB antagonist ANA-12 (15 μM) (Fig. 5B and 5D–E). Calcium release from internal stores is important for BDNF release (Dieni et al., 2012; Matsuda et al., 2009; Park et al., 2014). To test the requirement for calcium mobilization from internal stores in BDNF-induced BDNF release, we repeated the same experiment in the presence of the SERCA pump blocker cyclopiazonic acid (CPA, 30 μM for 30 min), which depletes calcium internal stores from the endoplasmic reticulum, and found that BDNF-induced BDNF release was abolished (Fig. 5C and 5D–E). Because exogenous BDNF application is known to potentiate MC-GC synaptic transmission and facilitate MC-induced burst firing of GCs (Hashimotodani et al., 2017), BDNF release from GC could result from postsynaptic firing (Brigadski and Lessmann, 2020). However, exogenous BDNF alone was not sufficient to increase GC firing (Fig. S2A and S2C), whereas subsequent blockade of inhibitory transmission by bath applying 100 μM picrotoxin robustly increased GC burst firing (Fig. S2A–C). Together, these findings demonstrate that BDNF is necessary and sufficient for BDNF secretion from GCs by mobilizing calcium from internal stores.

Enriched environment exposure induces BDNF-dependent LTP at MC-GC synapses *in vivo*

BDNF is commonly implicated in the neuronal and synaptic changes associated with exposure to an enriched environment (EE) (van Praag et al., 2000). There is good evidence that EE and voluntary exercise improve hippocampus-dependent learning (Bednarek and Caroni, 2011; Kempermann et al., 2010; van Praag et al., 2000), which likely relies on activity-dependent synaptic plasticity, and increase in BDNF/TrkB signaling (Foster and Dumas, 2001; Hosseiny et al., 2015; Ohline and Abraham, 2019). Given the essential role of BDNF/TrkB in MC-GC plasticity, we examined whether EE exposure potentiates MC-GC synaptic transmission in a BDNF-dependent manner. To test this possibility, we housed WT mice for 2 weeks in a cage with toys, running wheels, tunnels, and nests (Fig. 6B, enriched environment, EE) or in a standard cage (Fig. 6A, home cage, HC). We found that PPR and CV were decreased in EE mice compared to HC mice (Fig. 6C), consistent with an increase in evoked neurotransmitter release. In addition, we found that MC-GC LTP elicited by minimal stimulation in the IML (Fig. S3) was characterized with a significant increase in success rate, an increase in efficacy (i.e., mean EPSC amplitude including failures), and but no change in potency (i.e., mean EPSC amplitude excluding failures) (Fig. S3C). Remarkably, MC-GC LTP was abolished in *ex-vivo*, acute hippocampal slices obtained from EE as compared to HC mice (Fig. 6D). Although the duration of EE exposure likely induces different plasticity mechanisms, we found that one hour exposure to EE also reduced PPR and CV (Fig. 6E), and occluded MC-GC LTP (Fig. 6F). Together, these results strongly suggest that MC burst-induced LTP *in vitro* was occluded by the presynaptic strengthening of MC-GC transmission likely due to *in vivo* induction of MC-GC LTP after EE exposure.

Lastly, we sought to determine whether EE-induced potentiation of MC-GC synaptic transmission also requires BDNF/TrkB signaling, as observed in acute hippocampal slices. We therefore injected AAV5.CamKII.mCherry-Cre (*Bdnf* cKO) or AAV5.CamKII.mCherry (control) in the DG of 3–4 *Bdnf*$^{fl/fl}$ mice (Fig. 7A). One week post-surgery recovery, mice were placed in EE or HC for two weeks, and MC-GC EPSCs were then recorded from mCherry-positive GCs in acute hippocampal slices. Post-hoc analysis confirmed that Cre-mCherry and mCherry were expressed in both MCs and GCs (Fig. 7A). Consistent with our previous results, control mice exposed to EE showed reduced PPR and CV (Fig. 7B), and a failure in forskolin-induced LTP (Fig. 7C). In contrast, PPR and CV remained unchanged in *Bdnf* cKO mice exposed to EE and similar to HC (Fig. 7D), suggesting a failure in EE-mediated strengthening of MC-GC synaptic transmission. Because cAMP/PKA signaling is required for MC-GC LTP downstream BDNF/TrkB (Hashimotodani et al., 2017), we then examined whether cAMP/PKA activation could still induce MC-GC LTP in *Bdnf* cKO mice using forskolin. Forskolin (50 μM for 10 min) induced comparable

MC-GC potentiation in *Bdnf* cKO mice exposed to EE and HC (Fig. 7E). Taken together, our results show that BDNF/TrkB-dependent LTP can be triggered *in vivo* at MC-GC synapses, following EE exposure.

DISCUSSION

In this study, we report that presynaptic BDNF induces postsynaptic BDNF release and mediates a presynaptic form of LTP in the dentate gyrus. Specifically, burst stimulation of MC axons releases BDNF which, by activating postsynaptic TrkB, promotes BDNF release from GCs and triggers a long-lasting strengthening of MC-GC transmission (Fig. S4). In addition, we discovered that presynaptic CB_1R activity, which negatively controls MC-GC LTP induction, not only suppresses glutamate release from MC terminals (Chiu and Castillo, 2008; Jensen et al., 2021), but also inhibits activity-induced BDNF release. This inhibition likely accounts for the CB_1R-mediated dampening of BDNF/TrkB-dependent MC-GC LTP (Jensen et al., 2021). Lastly, we demonstrate that MC-GC LTP occurs *in vivo* following exposure to enrichment environment, via a BDNF-dependent mechanism. Taken together, our findings uncover novel mechanisms by which BDNF/TrkB signaling and presynaptic CB_1Rs can control synaptic function in the brain.

Despite many years of research on the role of BDNF/TrkB signaling in activity-dependent long-term plasticity (Bramham and Messaoudi, 2005; Brigadski and Lessmann, 2020; Edelmann et al., 2014; Lu et al., 2014; Park and Poo, 2013), a unified mechanism has not yet emerged. This is due at least in part to the mechanistically diverse forms of synaptic plasticity (Citri and Malenka, 2008; Monday et al., 2018), whether BDNF plays an instructive or regulatory (e.g., permissive) role, and the heterogenous effects on synaptic plasticity that result from interfering with BDNF release or TrkB signaling (Lu et al., 2014; Park and Poo, 2013). In addition, both the source of BDNF and the precise role of pre- and postsynaptic TrkB depends on the brain region, the brain developmental stage, the experimental conditions (e.g., *in vivo* versus *in vitro* studies, cultured neurons versus brain tissue), and the specific synapse and patterns of activity used to induce synaptic plasticity. Much of what we know about BDNF/TrkB signaling in synaptic plasticity derives from studies in the hippocampus, where diverse pre- and postsynaptic mechanisms have been identified. In the present study, we focused on the DG, a region of the hippocampal formation that contains one of the highest expression levels of BDNF within the mature brain (Conner et al., 1997; Yan et al., 1997b). Indeed, BDNF is highly expressed in GC proximal dendrites and MC

axon terminals (Conner et al., 1997; Dieni et al., 2012). While TrkB is expressed in GC dendrites, its presence in MC axons is less clear (Drake et al., 1999).

BDNF can act in an anterograde, retrograde, and paracrine manner (Brigadski and Lessmann, 2020; Edelmann et al., 2014). At the Schaffer collateral (Sch) to CA1 pyramidal neuron synapse, BDNF released from dendrites by a pairing protocol or glutamate uncaging anterogradely activates postsynaptic TrkB to mediate structural and functional postsynaptically-expressed LTP (Harward et al., 2016). A previous study showed that presynaptic, but not postsynaptic TrkB regulates Sch-CA1 LTP induced by high-frequency stimulation (Xu et al., 2000), while another study provided evidence that presynaptic BDNF release, presumably by activating TrkB on axon boutons, mediates a presynaptic component of Sch-CA1 LTP (Zakharenko et al., 2003). More recently, by genetically deleting BDNF or TrkB selectively in either CA3 or CA1 pyramidal neurons, it was reported that both anterograde and retrograde BDNF/TrkB signaling are implicated in the induction and maintenance of Sch-CA1 LTP, respectively (Lin et al., 2018). Unlike Sch-CA1 synapses (Lin et al., 2018), selective deletion of TrkB from MCs had no effect on MC-GC LTP (Fig. S1), strongly suggesting that presynaptically-expressed MC-GC LTP does not rely on retrograde signaling via presynaptic TrkB. In contrast, selective TrkB deletion from GCs impairs MC-GC LTP (Hashimotodani et al., 2017), indicating that postsynaptic TrkB activation is essential for this form of plasticity.

The DG contains one of the highest concentrations of BDNF within the brain (Conner et al., 1997; Dieni et al., 2012; Yan et al., 1997b). BDNF is expressed both in GC proximal dendrites, and in MC axon terminals present in the IML (Conner et al., 1997; Dieni et al., 2012; Yan et al., 1997b). At the MC-GC synapse, we found that presynaptic release of BDNF following physiologically-relevant burst stimulation of MC axons induced postsynaptic BDNF release from GCs in a postsynaptic TrkB-dependent manner. Moreover, BDNF was sufficient to induce postsynaptic BDNF release (Fig. 5A and 5D–E). Postsynaptic BDNF was necessary for synaptically-induced (Fig. 3D) but not forskolin-induced (Fig. 3E) potentiation, consistent with the fact that PKA signaling is engaged downstream of BDNF/TrkB cascade (Hashimotodani et al., 2017). In accordance with previous findings (Brigadski and Lessmann, 2020), BDNF-induced BDNF release required calcium release from internal stores (Fig. 5C–E). Together, our findings indicate that BDNF-induced BDNF release is an essential step for the induction of LTP at MC-GC synapses (Fig. S4), which does not require glutamatergic transmission (Jensen et al., 2021). A

similar mechanism could be implicated at other synapses expressing BDNF/TrkB-dependent plasticity.

To our knowledge, whether endogenous BDNF induces its own release to mediate synaptic plasticity in the mature brain was never demonstrated. An early study reported that exogenous application of neurotrophins (e.g., neurotrophin-3, neurotrophin-4/5, but not NGF) induces BDNF release in both cultured neurons and acute hippocampal slices, and this release depends on activation of neurotrophin receptors from the Trk family –as indicated by the kinase inhibitor K252a– and mobilization of calcium from internal stores (Canossa et al., 1997). This early observation suggested that neurotrophins can regulate their own secretion. BDNF-induced BDNF release could act as positive feedback that contributes to synaptic stabilization (Canossa et al., 1997), and axon initiation and growth during development (Cheng et al., 2011), but it could also play an instructive role for the induction of activity-dependent synaptic plasticity in the mature brain by increasing BDNF above critical concentrations. Here, we provide the first direct evidence that endogenous BDNF-induced BDNF release mediates activity-dependent LTP.

Common triggers of BDNF release include postsynaptic depolarization and the activation of metabotropic and ionotropic glutamate receptors (e.g., mGluR1/5 and NMDA receptors, respectively) (Brigadski and Lessmann, 2020; Lessmann et al., 2003; Park and Poo, 2013). However, MC-GC LTP can be induced in the absence of postsynaptic depolarization, glutamate release or activation of glutamate receptors (Hashimotodani et al., 2017; Jensen et al., 2021). BDNF can be released from dendrites upon action potential burst firing. For example, postsynaptic BDNF release following CA1 pyramidal cell theta-burst firing has been implicated in spike timing-dependent plasticity (Edelmann et al., 2015). In the DG, we recently found that GC theta-burst firing is sufficient to induce MC-GC LTP, and this plasticity is likely due to postsynaptic BDNF release as it is absent in mice where *Bdnf* was conditionally knocked out from GCs (Nasrallah et al., 2021a). Lastly, BDNF can also be released from astrocytes and microglia, and by this means contribute to synaptic plasticity (Brigadski and Lessmann, 2020). Nevertheless, our results using selective MC and GC BDNF cKO mice indicate that neuronal BDNF release induces MC-GC LTP, although a regulatory role of non-neuronal BDNF release cannot be excluded.

BDNF expression and release are highly regulated processes (Brigadski and Lessmann, 2020; Park and Poo, 2013). Consistent with the strong expression of CB_1Rs in MC axon terminals (Katona et al., 2006; Monory et al., 2006; Uchigashima et al., 2011), we found that CB_1R activity

negatively regulates presynaptic BDNF release from MC axons. In a recent study, we reported that tonic (i.e., ligand-independent) and phasic (i.e., cannabinoid-mediated) CB_1R activity reduces MC-GC synaptic transmission and dampens the induction of MC-GC LTP (Jensen et al., 2021). While the CB_1R-mediated reduction of glutamate release from MC boutons likely results from the suppression of presynaptic VGCCs via the βγ subunit, the mechanism underlying MC-GC LTP dampening was not determined. Here, we found that activity-dependent release of BDNF from MC axon terminals is suppressed by both tonic and phasic CB_1R activity (Fig. 2). Like for glutamate release, the CB_1R-mediated reduction of presynaptic BDNF release is presumably due to the suppression of presynaptic calcium influx via the βγ subunit, although a potential contribution due to cAMP/PKA reduction via the $\alpha_{i/o}$ subunit cannot be discarded given that BDNF secretion could be facilitated by intracellular cAMP (Cheng et al., 2011; Edelmann et al., 2015; Kolarow et al., 2007). By reducing presynaptic BDNF release from MC axons, CB_1Rs can control MC-GC synaptic strength in a long-term manner, thereby preventing runaway activity of the DG. Because BDNF promotes temporal lobe epilepsy (Lin et al., 2020; McNamara and Scharfman, 2012), and BDNF/TrkB-mediated MC-GC LTP facilitates early epileptogenesis (Nasrallah et al., 2021b), the CB_1R-mediated reduction of presynaptic BDNF release could be a mechanism by which cannabinoids may dampen epileptic activity. To the best of our knowledge, our study provides the first evidence that presynaptic CB_1Rs control the release of a neuropeptide, such as BDNF. Further analysis may reveal that CB_1R activity can control the release of other neuropeptides from CB_1R-expressing synapses.

Enrichment environment and exercise are known to promote BDNF expression in different brain areas including the dentate gyrus (Foster and Dumas, 2001; Hosseiny et al., 2015; Ohline and Abraham, 2019) and improve cognition (van Praag et al., 2000). We found that short (1 hour) and long (2 weeks) exposure to enriched environment strengthens MC-GC synaptic transmission in a presynaptic manner. PPR and CV were reduced and induction of MC-GC LTP (i.e., MC bursts or forskolin) was occluded, after exposure to enriched environment, consistent with the induction of MC-GC LTP *in vivo* (Fig. 6). In support of this possibility, knocking out *Bdnf* from hippocampal neurons abolished enriched environment-induced MC-GC synaptic strengthening (Fig. 7), strongly suggesting that induction of MC-GC LTP *in vivo* requires BDNF/TrkB signaling as described in acute hippocampal slices (this study and Hashimotodani et al., 2017). In addition, BDNF/TrkB signaling has emerged as a key factor that underlies neurological disorders such as epilepsy, depression, and anxiety (Minichiello, 2009; Wang et al., 2021). Molecular tools that

specifically target MCs or GCs in a subcellular compartment manner will be required to further characterize the precise involvement of BDNF arising from MCs and GCs *in vivo*.

FIGURE LEGENDS

Figure 1. Presynaptic BDNF expression and release is required for MC-GC LTP.

(A) Schematic diagram illustrating the optical stimulation of ChIEF-expressing MC axons and the recording configuration of GCs in contralateral hippocampal slices. A mix of AAV5.CaMKII.mCherry-Cre and AAV-DJ.FLEX.ChIEF-tdTomato was injected in the hilus of 3–4 w.o. *Bdnf*$^{fl/fl}$ (Pre *Bdnf* cKO) or WT (control) mice. Whole-cell patch-clamp recordings were performed from GCs in contralateral DG.

(B) Infrared/differential interference contrast (*left*) and fluorescence (*right*) images showing ChIEF-tdTomato was selectively expressed in the IML of contralateral DG of control and Pre *Bdnf* cKO mice.

(C) Summary plots showing PPR and CV were unchanged in Pre *Bdnf* cKO mice as compared to controls (PPR CTRL: 1.2 ± 0.04, n = 10; PPR cKO: 1.2 ± 0.05, n = 8; Control vs cKO, p = 0.7217, unpaired t-test; CV CTRL: 0.23 ± 0.04, n = 10; CV cKO: 0.19 ± 0.03, n = 8; Control vs cKO, p = 0.5654, Mann-Whitney's U test).

(D–E) Optically-induced LTP (Control: 167 ± 8.9% of baseline, n = 11, p < 0.001, paired t-test; Pre *Bdnf* cKO: 91 ± 7.4% of baseline, n = 8, p = 0.16363, paired t-test; Control vs cKO, p < 0.001, unpaired t-test), but not FSK-induced LTP (Control: 133 ± 8.1% of baseline, n = 4, p < 0.05, paired t-test; Pre *Bdnf* cKO: 143 ± 6.4% of baseline, n = 6, p < 0.01, paired t-test; Control vs cKO, p = 0.3441, unpaired t-test), was abolished in Pre *Bdnf* cKO mice as compared to controls. Arrows correspond to the burst-stimulation of MC axons (5 pulses, 100 Hz, repeated 50 times every 0.5 s). Representative traces (1) and (2) correspond to the areas (1) and (2) in the summary time-course plots. Data are represented as mean ± SEM. Number of cells and mice are showed between parentheses. n.s., not significant.

(F) Schematic diagram illustrating the injection of a mix of AAV5.CaMKII.mCherry-Cre and AAV-DJ.DIO.BDNF-pHluorin (BDNF-pH) in the hilus of 3–4 w.o. WT (control) mice.

(G) Experimental design of combined electrophysiology and 2-photon live imaging (2PLM) in acute hippocampal slices. Excitation wavelength employed was 880 nm. fEPSPs were performed using a stimulating pipette placed in the IML.

(H) 2-photon image showing BDNF-pH was selectively expressed in the IML of contralateral DG, likely in commissural MC axon terminals. Arrows indicate BDNF-pH puncta.

(I–J) Images showing changes in BDNF-pH fluorescence intensity after burst electrical stimulation of MC axon terminals in normal ACSF (**I**) or in the presence of VGGC inhibitor cadmium (100 μM, **J**).

(K) Time-course summary plot showing the average fractional fluorescence changes ($\Delta F/F_0$) over time.

(L) Quantification of the averaged responses 300–400 s following MC burst stimulation (Control: -0.28 ± 0.03, n = 6, $p < 0.01$, paired t-test; Cadmium: -0.04 ± 0.03, n = 6, $p = 0.3749$, paired t-test; Control vs Cadmium, $p < 0.001$, unpaired t-test). Data are represented as mean ± SEM. Number of slices and mice are showed between parentheses. ** $p < 0.01$; n.s., not significant.

Figure 2. Presynaptic BDNF release is under the control of CB_1R activity.

(A–B) Activation of CB_1Rs by pre-incubation with WIN 55,212-2 (5 μM, for 25 min) prevented changes of BDNF-pH fluorescence intensity after burst electrical stimulation of MC axon terminals. This effect was abolished in slices co-incubated with CB_1R inverse agonist AM251 (5 μM, for 25 min).

(C) Time-course summary plot showing the average fractional fluorescence changes ($\Delta F/F_0$) over time.

(D) Quantification of the averaged responses 300–400 s following MC burst stimulation (WIN: -0.08 ± 0.02, n = 6, $p = 0.0707$, paired t-test; WIN+AM251: -0.32 ± 0.05, n = 6, $p < 0.001$, paired t-test; WIN vs WIN+AM251, $p < 0.01$, unpaired t-test).

(E–F) A 30 Hz induction protocol was applied to induce submaximal LTP, and this protocol alone was not sufficient to induce significant BDNF release from MC axons. Inhibition of tonic CB_1Rs by bath application of AM251 (5 μM, for 25 min) decreases in BDNF-pH fluorescence intensity following submaximal LTP.

(G) Time-course summary plot showing the average fractional fluorescence changes ($\Delta F/F_0$) over time.

(H) Quantification of the averaged responses following 300–400 s MC burst stimulation (Submaximal LTP: -0.03 ± 0.01, n = 6, $p = 0.1216$, paired t-test; Submaximal LTP + AM251: -0.28 ± 0.03, n = 7, $p < 0.01$, paired t-test; Submaximal LTP vs Submaximal LTP + AM251, $p < 0.001$, unpaired t-test).

Data are represented as mean ± SEM. Number of slices and mice are showed between parentheses. *** $p < 0.001$; ** $p < 0.01$; n.s., not significant. Scale bar: 5 μm.

Figure 3. Postsynaptic BDNF is also required for MC-GC LTP.

(A) Schematic diagram illustrating the recording configuration of GCs from mCherry-positive GCs and the electrical stimulation of MC axons in ipsilateral hippocampal slices. AAV5.CaMKII.mCherry (control) or AAV5.CaMKII.mCherry-Cre (Post *Bdnf* cKO) was injected in the upper GCL of 3-4 w.o. *Bdnf*$^{fl/fl}$ mice. Whole-cell patch-clamp recordings were performed from mCherry-expressing GCs.

(B) Infrared/differential interference contrast (*left*) and fluorescence (*right*) images showing mCherry was sparsely expressed in the upper layer of GCL.

(C) Summary plots showing PPR (Control: 1.2 ± 0.03, n = 6; Post *Bdnf* cKO: 1.2 ± 0.05, n = 7; Control vs cKO, p = 0.3022, unpaired t-test) and CV (Control: 0.26 ± 0.05, n = 6; Post *Bdnf* cKO: 0.27 ± 0.06, n = 7; Control vs cKO, p = 0.16624, unpaired t-test) were unchanged in Post *Bdnf* cKO mice as compared to controls.

(D–E) Synaptically-induced LTP (Control: 158 ± 9% of baseline, n = 6, p < 0.01, paired t-test; Post *Bdnf* cKO: 100 ± 10% of baseline, n = 7, p = 0.9058, paired t-test; Control vs cKO, p < 0.01, unpaired t-test), but not FSK-induced LTP, was abolished in Post *Bdnf* cKO mice as compared to controls (Control: 142 ± 7% of baseline, n = 4, p < 0.01, paired t-test; Post *Bdnf* cKO: 138 ± 6% of baseline, n = 4, p < 0.01, paired t-test; Control vs cKO, p = 0.6959, unpaired t-test).

Arrows correspond to the burst-stimulation of MC axons (5 pulses, 100 Hz, repeated 50 times every 0.5 s). Representative traces (1) and (2) correspond to the areas (1) and (2) in the summary time course plots. Data are presented as mean ± SEM. Number of cells and animals are showed between parentheses. n.s., not significant.

Figure 4. Postsynaptic BDNF release is TrkB-dependent.

(A) Schematic diagram illustrating the injection of a mix of AAV5.CaMKII.mCherry-Cre and AAV-DJ.DIO.BDNF-pHluorin (BDNF-pH) in the hilus of 3–4 w.o. WT (control) mice.

(B) Experimental design of combined electrophysiology and 2PLM in acute hippocampal slices. Excitation wavelength employed was 880 nm. fEPSPs were performed using a stimulating pipette in the IML.

(C) 2-photon image showing BDNF-pH was selectively expressed in both GC soma and proximal dendrites. Arrows indicate BDNF-pH puncta.

(D–E) Images showing changes in BDNF-pH fluorescence intensity in GC proximal dendrites, after burst electrical stimulation of MC axon terminals in normal ACSF (**I**) or in the presence of a TrkB inhibitor ANA-12 (**J**).

(F) Time-course summary plot showing the average fractional fluorescence changes ($\Delta F/F_0$) over time.

(G) Quantification of the averaged responses 300–400 s following MC burst stimulation (Control: -0.23 ± 0.01, n = 7, p < 0.001, paired t-test; ANA-12: -0.02 ± 0.01% of baseline, n = 6, p = 0.0649, paired t-test; Control vs ANA-12, p < 0.001, unpaired t-test).

(H–I) *TrkB*$^{fl/fl}$ (Post *TrkB* cKO) and WT (control) littermates were injected with the same mix of viruses. 2-photon images showing changes in BDNF-pH fluorescence intensity in GC proximal dendrites, after burst electrical stimulation of MC axon terminals in WT (**H**) or Post *TrkB* cKO (**J**).

(J) Time-course summary plot showing the average fractional fluorescence changes ($\Delta F/F_0$) over time.

(K) Quantification of the averaged responses 300–400 s following MC burst stimulation (Control: -0.40 ± 0.02, n = 6, p < 0.01, Wilcoxon signed rank test; Post *TrkB* cKO: -0.07 ± 0.05% of baseline, n = 10, p = 0.1404, paired t-test; Control vs cKO, p < 0.01, Mann-Whitney's U test).

Data are represented as mean ± SEM. Number of slices and mice are showed between parentheses. *** p < 0.001; ** p < 0.01; * p < 0.05; n.s., not significant.

Figure 5. BDNF is sufficient to induce BDNF release by mobilizing calcium from internal stores.

(A–B) 2-photon images showing changes in BDNF-pH fluorescence intensity in GC proximal dendrites, following bath application of BDNF (8 nM) in normal ACSF (control, **A**) or in the presence of a TrkB inhibitor ANA-12 (**B**) or the SERCA pump blocker cyclopiazonic acid CPA (**C**).

(**D**) Time-course summary plot showing the average fractional fluorescence changes ($\Delta F/F_0$) over time.

(**E**) Quantification of the averaged responses 300–400 s following MC burst stimulation. BDNF (8 nM) decreases BDNF-pH fluorescent intensity (Control: -0.24 ± 0.02, n = 5, p < 0.01, paired t-test). This effect was abolished in the presence of 15 μM ANA-12 or 30 μM CPA (BDNF + ANA-12: -0.01 ± 0.01, n = 4, p = 0.6538, paired t-test; BDNF + CPA: -0.05 ± 0.02, n = 5, p = 0.0691, Wilcoxon signed rank test).

Data are represented as mean ± SEM. Number of slices and mice are showed between parentheses. ** p < 0.01; n.s., not significant.

Figure 6. Exposure to enriched environment strengthens MC-GC synapses and occludes LTP.

(A–B) Images showing the enriched environment (EE) compared to home cage (HC). WT mice were placed in the cage for 2 weeks (**C–D**) or 1 h (**E–F**).

(C and E) Summary plots showing that PPR (HC: 1.1 ± 0.07, n = 11; EE: 0.8 ± 0.05, n = 13; HC vs EE, $p < 0.01$, unpaired t-test) and CV (HC: 0.22 ± 0.02, n = 11; EE: 0.16 ± 0.01, n = 13; HC vs EE, $p < 0.05$, unpaired t-test) were decreased in mice exposed to EE during 2 weeks as compared to control HC mice. Similar results were observed following a 1-hour exposure (PPR HC: 1.2 ± 0.05, n = 9; PPR EE: 0.8 ± 0.05, n = 8; HC vs EE, $p < 0.001$, unpaired t-test; CV HC: 0.24 ± 0.02, n = 9; CV EE: 0.18 ± 0.01, n = 8; HC vs EE, $p < 0.05$, unpaired t-test).

(D and F) Synaptically-induced LTP was decreased in mice exposed to EE during 2 weeks as compared to controls (HC: 160 ± 19% of baseline, n = 7, $p < 0.05$, paired t-test; EE: 93 ± 6% of baseline, n = 10, $p = 0.0751$, paired t-test; HC vs EE: $p < 0.05$, unpaired t-test). Similar results were observed following 1-hour exposure to EE (HC: 165 ± 14% of baseline, n = 8, $p < 0.01$, paired t-test; EE: 114 ± 3% of baseline, n = 6, $p < 0.001$, paired t-test; HC vs EE: $p < 0.01$, unpaired t-test).

Data are represented as mean ± SEM. Number of slices and mice are showed between parentheses. *** $p < 0.001$; ** $p < 0.01$; * $p < 0.05$.

Figure 7. BDNF mediates activity-dependent LTP *in vivo*.

(A) BDNF was deleted from the DG by injecting an AAV5.CaMKII.mCherry (control) or AAV5.CaMKII.mCherry-Cre (*Bdnf* cKO) in the DG of 3–4 w.o. *Bdnf*$^{fl/fl}$ mice. After allowing mice to recover from surgery for 1 week, mice were placed in EE for 2 weeks. Acute hippocampal slices were prepared and whole-cell patch-clamp recordings were performed from mCherry-expressing GCs. Confocal images show mCherry and CRE-mCherry were expressed in both GCs and MCs.

(B) Summary plots showing that PPR and CV were reduced in control mice exposed to EE as compared to HC (PPR HC: 1.2 ± 0.07, n = 8; PPR EE: 0.8 ± 0.05, n = 7; HC vs EE, $p < 0.01$, unpaired t-test; CV HC: 0.28 ± 0.02, n = 8; CV EE: 0.16 ± 0.02, n = 7; HC vs EE, $p < 0.001$, unpaired t-test)**.**

(C) Forskolin (FSK)-induced LTP was abolished in EE-exposed mice as compared to controls (HC: 138 ± 8% of baseline, n = 5, $p < 0.05$, paired t-test; EE: 92 ± 6% of baseline, n = 5, $p = 0.2406$, paired t-test; HC vs EE, $p < 0.01$, unpaired t-test).

(D) No changes in PPR and CV were observed in *Bdnf* cKO mice exposed to HC or EE (PPR HC: 1.2 ± 0.04, n = 7; PPR EE: 1.2 ± 0.07, n = 9; HC vs EE, $p = 0.86$, unpaired t-test; CV HC: 0.25 ± 0.03, n = 7; CV EE: 0.26 ± 0.03, n = 9; HC vs EE, $p = 0.84413$, unpaired t-test). Summary plots are showed.

(E) FSK-induced LTP was intact in *Bdnf* cKO mice after HC or EE exposure (HC: 161 ± 15% of baseline, n = 6, $p < 0.05$, paired t-test; EE: 148 ± 10% of baseline, n = 5, $p < 0.01$, paired t-test; HC vs EE, $p = 0.5196$, unpaired t-test).

Data are represented as mean ± SEM. Number of slices and mice are showed between parentheses. *** $p < 0.001$; ** $p < 0.01$; n.s., not significant.

SUPPLEMENTAL FIGURE LEGENDS

Figure S1 (related to Fig. 4). Presynaptic TrkB is not required for MC-GC LTP.

(A) Schematic diagram illustrating the optical stimulation of ChIEF-expressing MC axons and the recording configuration of GCs in contralateral hippocampal slices. A mix of AAV5.CaMKII.mCherry-Cre and AAV-DJ.FLEX.ChIEF-tdTomato was injected in the hilus of 3–4 w.o. WT (control) or *TrkB*$^{fl/fl}$ (Pre *TrkB* cKO) mice. Whole-cell patch-clamp recordings were performed from GCs in contralateral DG.

(B) Infrared/differential interference contrast (*left*) and fluorescence (*right*) images showing ChIEF-tdTomato was selectively expressed in the IML of contralateral DG of control and Pre *TrkB* cKO mice.

(C) Optically-induced LTP was intact in Pre *TrkB* cKO mice as compared to controls (Control: 152 ± 11% of baseline, n = 7, $p < 0.01$, paired t-test; Pre *TrkB* cKO: 159 ± 12% of baseline, n = 5, $p < 0.01$, paired t-test; Control vs cKO, $p = 0.6767$, unpaired t-test). Arrows correspond to the burst-stimulation of MC axons. Representative traces (1) and (2) correspond to the areas (1) and (2) in the summary time-course plots. Data are represented as mean ± SEM. Number of cells and mice are showed between parentheses.

Figure S2 (related to Fig. 5). BDNF alone does not trigger GC firing.

(A) Sample traces of two representative experiments showing burst stimulation before and after application of BDNF (8 nM) or picrotoxin (100 μM).

(B) Time-course plot (representative experiment) of the number of spikes per burst in the presence of 8 nM BDNF and 100 μM picrotoxin.

(C) Summary data showing the spike probability after bath application of BDNF and picrotoxin in the same GC (spike probability in picrotoxin: 49 ± 5%, n = 4; baseline vs picrotoxin, $p < 0.01$, Wilcoxon signed rank test).

Figure S3 (related to Fig. 6). Enriched environment-induced MC-GC LTP is presynaptically expressed.

(A–B) Time-course plot (representative experiment) of the minimal stimulation in IML of WT mice exposed to HC or EE for 2 weeks.

(C) Sample traces (top) and time course plot (bottom) showing EE mice are characterized by a significant increase in success rate (HC: 36 ± 2.8%, n = 15; EE: 48 ± 4%, n = 12; $p < 0.05$, unpaired t test), an increase in efficacy (HC: -5.5 ± 0.5 pA, n = 15; EE: -8.5 ± 1.2 pA, n = 12; $p < 0.01$; Mann-Whitney's U test), and no change in potency (HC: -13.2 ± 1.4 pA, n = 15; EE: -15.4 ± 1.7 pA, n = 12, $p = 0.17$; Mann-Whitney's U test).

Figure S4 (related to Fig. 1–7). Working model.

Repetitive activity of MC axons releases BDNF, which by activating postsynaptic TrkB likely mobilizes calcium internal stores and induces postsynaptic BDNF secretion (i.e., from GCs) and MC-GC synaptic strengthening. In addition, CB_1R activity tightly inhibits presynaptic BDNF, thereby controls MC-GC synaptic strengthening.

METHODS

Experimental model and subject details

C57BL/6J (Charles River), floxed-*Bdnf* (*Bdnf*$^{fl/fl}$) or floxed-*Trkb* (*TrkB*$^{fl/fl}$) mice of either sex were used for electrophysiological and imaging experiments. All animals were group housed in a standard 12 h. light/12 h. dark cycle. Animal handling and use followed a protocol approved by the Animal Care and Use Committee of Albert Einstein College of Medicine, in accordance with the National Institutes of Health guidelines. *Bdnf*$^{fl/fl}$ and *TrkB*$^{fl/fl}$ mice were generously donated by Dr. Lisa Monteggia at the University of Texas (Southwestern Medical Center).

Presynaptic *Bdnf* and *TrkB* conditional knockout combined to optogenetics

A mix of Cre recombinase-containing adeno-associated viruses AAV5.CamKII.mCherry-Cre (University of Pennsylvania Vector Core) and Cre-dependent ChiEF (AAV-DJ.FLEX.ChiEF-tdTomato) was injected into the DG of 3–4 weeks old (w.o.) *Bdnf*$^{fl/fl}$, *TrkB*$^{fl/fl}$. WT littermates injected with the same viruses served as controls. The mix of viruses (1 µL total, 1:2 ratio) was injected at a rate of 0.1 µL/min unilaterally into the DG (2.18 mm posterior to bregma, 1.5 mm lateral to bregma, 2.20 mm ventral from dura, for 4.2-mm lambda-bregma distance) of *Bdnf*$^{fl/fl}$, *TrkB*$^{fl/fl}$ or WT mice. All coordinates were adjusted to the lambda-bregma distance for each animal. Briefly, animals were placed on a stereotaxic apparatus (Kopf Instruments) and anesthetized with isoflurane (5% for induction and 1.5% for maintenance). Slices for electrophysiology were prepared from injected animals 4–5 weeks after surgery. This strategy allowed us to optically activate Cre-positive commissural MC axons and record from GCs in the contralateral hippocampus. For each animal, we verified the presence of tdTomato-expressing, putative MC axon terminals in the IML of contralateral slices.

Postsynaptic *Bdnf* and *TrkB* conditional knockout

AAV5.CamKII.mCherry (control) or AAV5.CamKII.Cre-mCherry (University of Pennsylvania Vector Core) were injected (1 µL, flow rate of 0.1 µL/min) bilaterally into the upper blade of the DG (2.06 mm posterior to bregma, ± 1.5 mm lateral to bregma, 1.65 mm ventral from dura) of 3–4 w.o. *Bdnf*$^{fl/fl}$ or *TrkB*$^{fl/fl}$. Slices for electrophysiology were prepared from injected animals 10 days after surgery. For each animal, we verified the absence of mCherry-expressing cells in the hilus of the whole ipsilateral hippocampus.

Hippocampal slice preparation

Acute transverse hippocampal slices (300-µm thick) were prepared from *Bdnf*$^{fl/fl}$, *TrkB*$^{fl/fl}$ or WT mice, for electrophysiology or imaging experiments. Briefly, the hippocampi were isolated and cut using a VT1200s microsclicer (Leica Microsystems Co.) in an ice-cold cutting solution containing (in mM): 110 choline, 2.5 KCl, 25 $NaHCO_3$, 1.25 NaH_2PO_4, 0.5 $CaCl_2$, 7 $MgCl_2$, 25 D-glucose, 11.6 sodium L-ascorbate, and 3.1 sodium pyruvate. Slices were then transferred and incubated for 30 min in a chamber placed in a warm bath (33–34°C) with extracellular artificial cerebrospinal fluid (ACSF) solution containing (in mM): 124 NaCl, 2.5 KCl, 26 $NaHCO_3$, 1 NaH_2PO_4, 2.5 $CaCl_2$, 1.3 $MgSO_4$ and 10 D-glucose. Slices were kept at room temperature for at least 30 min prior to experiments. All solutions were equilibrated with 95% O2 and 5% CO2 (pH 7.4).

Electrophysiology

All recordings were performed at 28 ± 1°C in a submersion-type recording chamber perfused at 2 mL/min with ACSF supplemented with the $GABA_A$ receptor antagonist picrotoxin (100 μM). Whole-cell patch-clamp recordings using a Multiclamp 700A amplifier (Molecular Devices) were made from GCs voltage clamped at −60 mV using patch-type pipette electrodes (~3–4 MΩ) containing (in mM): 131 cesium gluconate, 8 NaCl, 1 CaCl2, 10 EGTA, 10 D-glucose, and 10 HEPES (pH 7.2, 285-290 mOsm). For Fig. S2, whole-cell patch-clamp recordings were made using K^+-based internal solution, containing the following intracellular solution (in mM): 135 $KMeSO_4$, 5 KCl, 1 $CaCl_2$, 5 NaOH, 10 HEPES, 5 MgATP, 0.4 Na_3GTP, 5 EGTA and 10 D-glucose, pH 7.2 (280-290 mOsm). Series resistance (~7–28 MΩ) was monitored throughout all experiments with a −5 mV, 80 ms voltage step, and cells that exhibited a significant change in series resistance (> 20%) were excluded from analysis. All experiments were performed in an interleaved fashion –i.e., control experiments were performed every test experiment on the same day.

A stimulating patch-type pipette filled with ACSF was placed in the IML (< 30 μm from the border of the GC body layer) to activate MC axons. To elicit synaptic responses, paired, monopolar square-wave voltage or current pulses (100–200 μs pulse width, 4–25 V) were delivered through a stimulus isolator (Isoflex, AMPI). Typically, stimulation intensity was adjusted to obtain comparable magnitude synaptic responses across experiments (e.g., 50–100 pA EPSCs at V_h −60 mV). MC-GC LTP was induced with brief bursts (5 pulses, 100 Hz) repeated 50 times at 2 Hz (for a total of 25 seconds) while postsynaptic neurons were continuously voltage-clamped at −60 mV.

Electrophysiological data were acquired at 5 kHz, filtered at 2.4 kHz, and analyzed using custom-made software for IgorPro 7.01 (Wavemetrics, Inc.). The magnitude of LTP was determined by comparing 10 min baseline responses with responses 20–30 min after LTP induction or forskolin-induced potentiation. PPR was defined as the ratio of the amplitude of the second EPSC, to the amplitude of the first EPSC. CV was calculated as the standard deviation of EPSC amplitude divided by the mean of EPSC amplitude. Both PPR and CV were measured during 10-min baseline. Averaged traces include 20 consecutive individual responses.

Optogenetics

At least 4 weeks post-surgery, acute hippocampal slices were prepared as previously described and slices showing optimal tdTomato expression in the IML of the contralateral DG were used for electrophysiology. Pulses of blue light (0.5−2 ms width duration) were provided using a 473-nm LED (ThorLabs, Inc.) through the microscope objective (40x, 0.8 NA) and centered in the IML.

Two-photon BDNF-pHluorin imaging

A mix of Cre recombinase-containing virus (AAV5.CamKII.mCherry-Cre) and Cre-dependent BDNF-pHluorin (AAV-DJ.DIO.BDNF-pHluorin) was injected into the DG of 3–4 weeks old WT or *TrkB*$^{fl/fl}$ mice. To measure presynaptic BDNF release, the mix of viruses (1 μL total, 1:2 ratio) was injected at a flow rate of 0.1 μL/min unilaterally into the hilus (2.18 mm posterior to bregma, 1.5 mm lateral to bregma, 2.20 mm ventral from dura, for 4.2-mm lambda-bregma distance). To

measure postsynaptic BDNF release, the mix was injected bilaterally into the upper GCL (2.06 mm posterior to bregma, ± 1.5 mm lateral to bregma, 1.65 mm ventral from dura) to avoid expression in MCs. Acute hippocampal slices were prepared as previously described and slices showing optimal mCherry expression were taken for imaging sessions.

All imaging experiments were performed in a submersion-type recording chamber perfused at 2 mL/min with ACSF. Briefly, a broken tip stimulating pipette was placed in the IML at least 100 µm away from the imaging site. Extracellular field recordings were monitored simultaneously using a patch-type pipette filled with 1 M NaCl and placed in IML. The Insight Deep See laser (Spectra Physics) was tuned to 880 nm and the imaging site was selected by the appearance of BDNF-pH puncta in the IML. Using 512 X 512 pixel resolution, the region of interest (ROI) was magnified to 6–8 X and a baseline acquisition of 40 consecutive images at 0.2 Hz was acquired using T-series software (PrairieView 5.4, Bruker Corp.). Following baseline acquisition, a brief MC burst-stimulation (5 pulses at 100 Hz, repeated 50 times at 2 Hz) was delivered and at least 80 consecutive images were acquired at 0.2 Hz. To verify reactivity of the ROI an isosmotic solution of NH_4Cl (50 mM) was added at the end of the imaging session as previously reported (Park et al., 2014). ROIs were defined manually for each experiment, blind to the injection conditions or treatments. The ROI fluorescence intensity was measured, and the $\Delta F/F_0$ of BDNF-pH signal was determined, using ImageJ software.

Enriched Environment

Standard mouse cages (28 cm x 18 cm) containing a feeder and a water dispenser were used as home cages (HC). Enriched environment (EE) housing consists in a large cage (121 cm x 61 cm) containing a feeder, a water dispenser, multiple running wheels, plastic tubes, domes, and other plastic toys (Fig. 6A–B). Objects were moved every day to maintain novelty. EE refers to both the effects of cognitive enrichment strictly defined (i.e., exploration, toys, large area), as well as exercise on running wheels. Experimenters were blind to condition when performing and analyzing experiments.

Reagents

Reagents were bath applied following dilution into ACSF from stock solutions stored at −4°C or −20°C prepared in water or DMSO, depending on the manufacturer's recommendation. The final DMSO concentration was < 0.01% total volume. Reagents *N*-(piperidin-1-yl)-5-(4-iodophenyl)-1-(2,4-dichlorophenyl)-4-methyl-1*H*-pyrazole-3-carboxamide (AM251), (*R*)-(+)-[2,3-Dihydro-5-methyl-3-(4-morpholinylmethyl)pyrrolo[1,2,3-*de*]-1,4-benzoxazin-6-yl]-1-naphthalenylmethanone mesylate (WIN 55,212-2), *N*-[2-[[(Hexahydro-2-oxo-1*H*-azepin-3-yl)amino]carbonyl]phenyl]benzo[b]thiophene-2-carboxamide (ANA-12), forskolin, cyclopiazonic acid and picrotoxin were purchased from Tocris Bioscience. Dimethyl Sulfoxide (DMSO) and cadmium were purchased from Sigma-Aldrich. Recombinant human BDNF protein was purchased from Hello Bio. Salts for making ACSF and internal solutions were purchased from Sigma-Aldrich.

Quantification and Statistical Analysis

Statistical analysis was performed using OriginPro software (OriginLab b9.2.272). For imaging, analysis was done blind to the conditions. The normality of distributions was assessed using the Shapiro-Wilk test. In normal distributions, Student's unpaired and paired two-tailed t-tests were used to assess between-group and within-group differences, respectively. The non-parametric paired sample Wilcoxon signed rank test and Mann-Whitney's U test were used in non-normal distributions. Statistical significance was set to $p < 0.05$ (*** indicates $p < 0.001$, ** indicates $p < 0.01$, and * indicates $p < 0.05$).

Acknowledgements

We thank all the Castillo lab members for discussion. We thank Drs. P. Kaeser and H. Park (Korea Brain Research Institute) for providing pAAV-FLEX-ChIEF-tdTomato and pAAV-DIO-BDNF-pHluorin, respectively. We also thank Dr. Lisa Monteggia (University of Texas, Southwestern Medical Center) for providing TrkB-floxed and BDNF-floxed mice. This research was supported by the National Institutes of Health (R01-MH081935, R01-DA17392 and R01-NS113600) to P.E.C., a Junior Investigator Neuroscience Research Award (Einstein) to C.B and an American Epilepsy Society award to K.N. Confocal images were obtained at the Einstein Imaging Core (supported by The Rose F Kennedy Intellectual Disabilities Research Center - shared instrument grant 1S10OD25295 to Konstantin Dobrenis).

Author Contributions

C.B. and P.E.C. designed the experiments. C.B. performed and analyzed electrophysiological recordings and imaging. K.N. performed preliminary data that lead to this study and minimal stimulation experiments. C.B. and P.E.C. wrote the manuscript with inputs from K.N.

The authors declare no conflict of interest.

REFERENCES

Amaral, D.G., Scharfman, H.E., and Lavenex, P. (2007). The dentate gyrus: fundamental neuroanatomical organization (dentate gyrus for dummies). Prog Brain Res *163*, 3-22.

Bednarek, E., and Caroni, P. (2011). beta-Adducin is required for stable assembly of new synapses and improved memory upon environmental enrichment. Neuron *69*, 1132-1146.

Bramham, C.R., and Messaoudi, E. (2005). BDNF function in adult synaptic plasticity: the synaptic consolidation hypothesis. Prog Neurobiol *76*, 99-125.

Brigadski, T., and Lessmann, V. (2020). The physiology of regulated BDNF release. Cell Tissue Res *382*, 15-45.

Buckmaster, P.S., and Soltesz, I. (1996). Neurobiology of hippocampal interneurons: a workshop review. Hippocampus *6*, 330-339.

Canossa, M., Griesbeck, O., Berninger, B., Campana, G., Kolbeck, R., and Thoenen, H. (1997). Neurotrophin release by neurotrophins: implications for activity-dependent neuronal plasticity. Proc Natl Acad Sci U S A *94*, 13279-13286.

Castillo, P.E., Younts, T.J., Chavez, A.E., and Hashimotodani, Y. (2012). Endocannabinoid signaling and synaptic function. Neuron *76*, 70-81.

Cheng, P.L., Song, A.H., Wong, Y.H., Wang, S., Zhang, X., and Poo, M.M. (2011). Self-amplifying autocrine actions of BDNF in axon development. Proc Natl Acad Sci U S A *108*, 18430-18435.

Chiu, C.Q., and Castillo, P.E. (2008). Input-specific plasticity at excitatory synapses mediated by endocannabinoids in the dentate gyrus. Neuropharmacology *54*, 68-78.

Citri, A., and Malenka, R.C. (2008). Synaptic plasticity: multiple forms, functions, and mechanisms. Neuropsychopharmacology *33*, 18-41.

Conner, J.M., Lauterborn, J.C., Yan, Q., Gall, C.M., and Varon, S. (1997). Distribution of brain-derived neurotrophic factor (BDNF) protein and mRNA in the normal adult rat CNS: evidence for anterograde axonal transport. The Journal of neuroscience : the official journal of the Society for Neuroscience *17*, 2295-2313.

Dieni, S., Matsumoto, T., Dekkers, M., Rauskolb, S., Ionescu, M.S., Deogracias, R., Gundelfinger, E.D., Kojima, M., Nestel, S., Frotscher, M.*, et al.* (2012). BDNF and its pro-peptide are stored in presynaptic dense core vesicles in brain neurons. The Journal of cell biology *196*, 775-788.

Donovan, M.H., Yamaguchi, M., and Eisch, A.J. (2008). Dynamic expression of TrkB receptor protein on proliferating and maturing cells in the adult mouse dentate gyrus. Hippocampus *18*, 435-439.

Drake, C.T., Milner, T.A., and Patterson, S.L. (1999). Ultrastructural localization of full-length trkB immunoreactivity in rat hippocampus suggests multiple roles in modulating activity-dependent synaptic plasticity. The Journal of neuroscience : the official journal of the Society for Neuroscience *19*, 8009-8026.

Edelmann, E., Cepeda-Prado, E., Franck, M., Lichtenecker, P., Brigadski, T., and Lessmann, V. (2015). Theta Burst Firing Recruits BDNF Release and Signaling in Postsynaptic CA1 Neurons in Spike-Timing-Dependent LTP. Neuron *86*, 1041-1054.

Edelmann, E., Lessmann, V., and Brigadski, T. (2014). Pre- and postsynaptic twists in BDNF secretion and action in synaptic plasticity. Neuropharmacology *76 Pt C*, 610-627.

Foster, T.C., and Dumas, T.C. (2001). Mechanism for increased hippocampal synaptic strength following differential experience. J Neurophysiol *85*, 1377-1383.

Gangarossa, G., Perez, S., Dembitskaya, Y., Prokin, I., Berry, H., and Venance, L. (2020). BDNF Controls Bidirectional Endocannabinoid Plasticity at Corticostriatal Synapses. Cereb Cortex *30*, 197-214.

Harward, S.C., Hedrick, N.G., Hall, C.E., Parra-Bueno, P., Milner, T.A., Pan, E., Laviv, T., Hempstead, B.L., Yasuda, R., and McNamara, J.O. (2016). Autocrine BDNF-TrkB signalling within a single dendritic spine. Nature *538*, 99-103.

Hashimotodani, Y., Nasrallah, K., Jensen, K.R., Chavez, A.E., Carrera, D., and Castillo, P.E. (2017). LTP at Hilar Mossy Cell-Dentate Granule Cell Synapses Modulates Dentate Gyrus Output by Increasing Excitation/Inhibition Balance. Neuron *95*, 928-943 e923.

Hosseiny, S., Pietri, M., Petit-Paitel, A., Zarif, H., Heurteaux, C., Chabry, J., and Guyon, A. (2015). Differential neuronal plasticity in mouse hippocampus associated with various periods of enriched environment during postnatal development. Brain Struct Funct *220*, 3435-3448.

Inagaki, T., Begum, T., Reza, F., Horibe, S., Inaba, M., Yoshimura, Y., and Komatsu, Y. (2008). Brain-derived neurotrophic factor-mediated retrograde signaling required for the induction of long-term potentiation at inhibitory synapses of visual cortical pyramidal neurons. Neurosci Res *61*, 192-200.

Jakawich, S.K., Nasser, H.B., Strong, M.J., McCartney, A.J., Perez, A.S., Rakesh, N., Carruthers, C.J., and Sutton, M.A. (2010). Local presynaptic activity gates homeostatic changes in presynaptic function driven by dendritic BDNF synthesis. Neuron *68*, 1143-1158.

Jensen, K.R., Berthoux, C., Nasrallah, K., and Castillo, P.E. (2021). Multiple cannabinoid signaling cascades powerfully suppress recurrent excitation in the hippocampus. Proc Natl Acad Sci U S A *118*.

Jinde, S., Zsiros, V., Jiang, Z., Nakao, K., Pickel, J., Kohno, K., Belforte, J.E., and Nakazawa, K. (2012). Hilar mossy cell degeneration causes transient dentate granule cell hyperexcitability and impaired pattern separation. Neuron *76*, 1189-1200.

Katona, I., Urban, G.M., Wallace, M., Ledent, C., Jung, K.M., Piomelli, D., Mackie, K., and Freund, T.F. (2006). Molecular composition of the endocannabinoid system at glutamatergic synapses. The Journal of neuroscience : the official journal of the Society for Neuroscience *26*, 5628-5637.

Kempermann, G., Fabel, K., Ehninger, D., Babu, H., Leal-Galicia, P., Garthe, A., and Wolf, S.A. (2010). Why and how physical activity promotes experience-induced brain plasticity. Front Neurosci *4*, 189.

Kesner, R.P., and Rolls, E.T. (2015). A computational theory of hippocampal function, and tests of the theory: new developments. Neurosci Biobehav Rev *48*, 92-147.

Kolarow, R., Brigadski, T., and Lessmann, V. (2007). Postsynaptic secretion of BDNF and NT-3 from hippocampal neurons depends on calcium calmodulin kinase II signaling and proceeds via delayed fusion pore opening. The Journal of neuroscience : the official journal of the Society for Neuroscience *27*, 10350-10364.

Korte, M., Kang, H., Bonhoeffer, T., and Schuman, E. (1998). A role for BDNF in the late-phase of hippocampal long-term potentiation. Neuropharmacology *37*, 553-559.

Lemtiri-Chlieh, F., and Levine, E.S. (2010). BDNF evokes release of endogenous cannabinoids at layer 2/3 inhibitory synapses in the neocortex. J Neurophysiol *104*, 1923-1932.

Lessmann, V., Gottmann, K., and Malcangio, M. (2003). Neurotrophin secretion: current facts and future prospects. Prog Neurobiol *69*, 341-374.

Lin, P.Y., Kavalali, E.T., and Monteggia, L.M. (2018). Genetic Dissection of Presynaptic and Postsynaptic BDNF-TrkB Signaling in Synaptic Efficacy of CA3-CA1 Synapses. Cell Rep *24*, 1550-1561.

Lin, T.W., Harward, S.C., Huang, Y.Z., and McNamara, J.O. (2020). Targeting BDNF/TrkB pathways for preventing or suppressing epilepsy. Neuropharmacology *167*, 107734.

Liu, Y., Zhang, L.I., and Tao, H.W. (2007). Heterosynaptic scaling of developing GABAergic synapses: dependence on glutamatergic input and developmental stage. The Journal of neuroscience : the official journal of the Society for Neuroscience *27*, 5301-5312.

Lu, B., Nagappan, G., and Lu, Y. (2014). BDNF and synaptic plasticity, cognitive function, and dysfunction. Handb Exp Pharmacol *220*, 223-250.

Matsuda, N., Lu, H., Fukata, Y., Noritake, J., Gao, H., Mukherjee, S., Nemoto, T., Fukata, M., and Poo, M.M. (2009). Differential activity-dependent secretion of brain-derived neurotrophic factor from axon and dendrite. The Journal of neuroscience : the official journal of the Society for Neuroscience *29*, 14185-14198.

McNamara, J.O., and Scharfman, H.E. (2012). Temporal Lobe Epilepsy and the BDNF Receptor, TrkB. In Jasper's Basic Mechanisms of the Epilepsies, th, J.L. Noebels, M. Avoli, M.A. Rogawski, R.W. Olsen, and A.V. Delgado-Escueta, eds. (Bethesda (MD)).

Minichiello, L. (2009). TrkB signalling pathways in LTP and learning. Nature Reviews Neuroscience *10*, 850-860.

Minichiello, L., Korte, M., Wolfer, D., Kühn, R., Unsicker, K., Cestari, V., Rossi-Arnaud, C., Lipp, H.-P., Bonhoeffer, T., and Klein, R. (1999). Essential Role for TrkB Receptors in Hippocampus-Mediated Learning. Neuron *24*, 401-414.

Monday, H.R., Younts, T.J., and Castillo, P.E. (2018). Long-Term Plasticity of Neurotransmitter Release: Emerging Mechanisms and Contributions to Brain Function and Disease. Annu Rev Neurosci *41*, 299-322.

Monory, K., Massa, F., Egertova, M., Eder, M., Blaudzun, H., Westenbroek, R., Kelsch, W., Jacob, W., Marsch, R., Ekker, M.*, et al.* (2006). The endocannabinoid system controls key epileptogenic circuits in the hippocampus. Neuron *51*, 455-466.
Nasrallah, K., Berthoux, C., Hashimotodani, Y., Chavez, A.E., Gulfo, M., Luján, R., and Castillo, P.E. (2021a). Retrograde adenosine/A2A receptor signaling mediates presynaptic hippocampal LTP and facilitates epileptic seizures. bioRxiv.
Nasrallah, K., Frechou, M.A., Yoon, J.Y., Persaud, S., Gonçalvez, T., and Castillo, P.E. (2021b). Activity-dependent LTP in the dentate gyrus promotes epileptic seizures. bioRxiv.
Ohline, S.M., and Abraham, W.C. (2019). Environmental enrichment effects on synaptic and cellular physiology of hippocampal neurons. Neuropharmacology *145*, 3-12.
Park, H. (2018). Cortical Axonal Secretion of BDNF in the Striatum Is Disrupted in the Mutant-huntingtin Knock-in Mouse Model of Huntington's Disease. Exp Neurobiol *27*, 217-225.
Park, H., and Poo, M.M. (2013). Neurotrophin regulation of neural circuit development and function. Nat Rev Neurosci *14*, 7-23.
Park, H., Popescu, A., and Poo, M.-m. (2014). Essential role of presynaptic NMDA receptors in activity-dependent BDNF secretion and corticostriatal LTP. Neuron *84*, 1009-1022.
Rolls, E.T. (2013). The mechanisms for pattern completion and pattern separation in the hippocampus. Front Syst Neurosci *7*, 74.
Sasi, M., Vignoli, B., Canossa, M., and Blum, R. (2017). Neurobiology of local and intercellular BDNF signaling. Pflugers Arch *469*, 593-610.
Scharfman, H.E. (2016). The enigmatic mossy cell of the dentate gyrus. Nat Rev Neurosci *17*, 562-575.
Shimojo, M., Courchet, J., Pieraut, S., Torabi-Rander, N., Sando, R., 3rd, Polleux, F., and Maximov, A. (2015). SNAREs Controlling Vesicular Release of BDNF and Development of Callosal Axons. Cell Rep *11*, 1054-1066.
Uchigashima, M., Yamazaki, M., Yamasaki, M., Tanimura, A., Sakimura, K., Kano, M., and Watanabe, M. (2011). Molecular and morphological configuration for 2-arachidonoylglycerol-mediated retrograde signaling at mossy cell-granule cell synapses in the dentate gyrus. The Journal of neuroscience : the official journal of the Society for Neuroscience *31*, 7700-7714.
van Praag, H., Kempermann, G., and Gage, F.H. (2000). Neural consequences of environmental enrichment. Nat Rev Neurosci *1*, 191-198.
Wang, C.S., Kavalali, E.T., and Monteggia, L.M. (2021). BDNF signaling in context: From synaptic regulation to psychiatric disorders. Cell.
Wu, Y., Liu, Q., Guo, B., Ye, F., Ge, J., and Xue, L. (2020). BDNF Activates Postsynaptic TrkB Receptors to Induce Endocannabinoid Release and Inhibit Presynaptic Calcium Influx at a Calyx-Type Synapse. The Journal of neuroscience : the official journal of the Society for Neuroscience *40*, 8070-8087.
Xu, B., Gottschalk, W., Chow, A., Wilson, R.I., Schnell, E., Zang, K., Wang, D., Nicoll, R.A., Lu, B., and Reichardt, L.F. (2000). The role of brain-derived neurotrophic factor receptors in the mature hippocampus: modulation of long-term potentiation through a presynaptic mechanism involving TrkB. The Journal of neuroscience : the official journal of the Society for Neuroscience *20*, 6888-6897.
Yan, Q., Radeke, M.J., Matheson, C.R., Talvenheimo, J., Welcher, A.A., and Feinstein, S.C. (1997a). Immunocytochemical localization of TrkB in the central nervous system of the adult rat. J Comp Neurol *378*, 135-157.
Yan, Q., Rosenfeld, R.D., Matheson, C.R., Hawkins, N., Lopez, O.T., Bennett, L., and Welcher, A.A. (1997b). Expression of brain-derived neurotrophic factor protein in the adult rat central nervous system. Neuroscience *78*, 431-448.
Zakharenko, S.S., Patterson, S.L., Dragatsis, I., Zeitlin, S.O., Siegelbaum, S.A., Kandel, E.R., and Morozov, A. (2003). Presynaptic BDNF required for a presynaptic but not postsynaptic component of LTP at hippocampal CA1-CA3 synapses. Neuron *39*, 975-990.

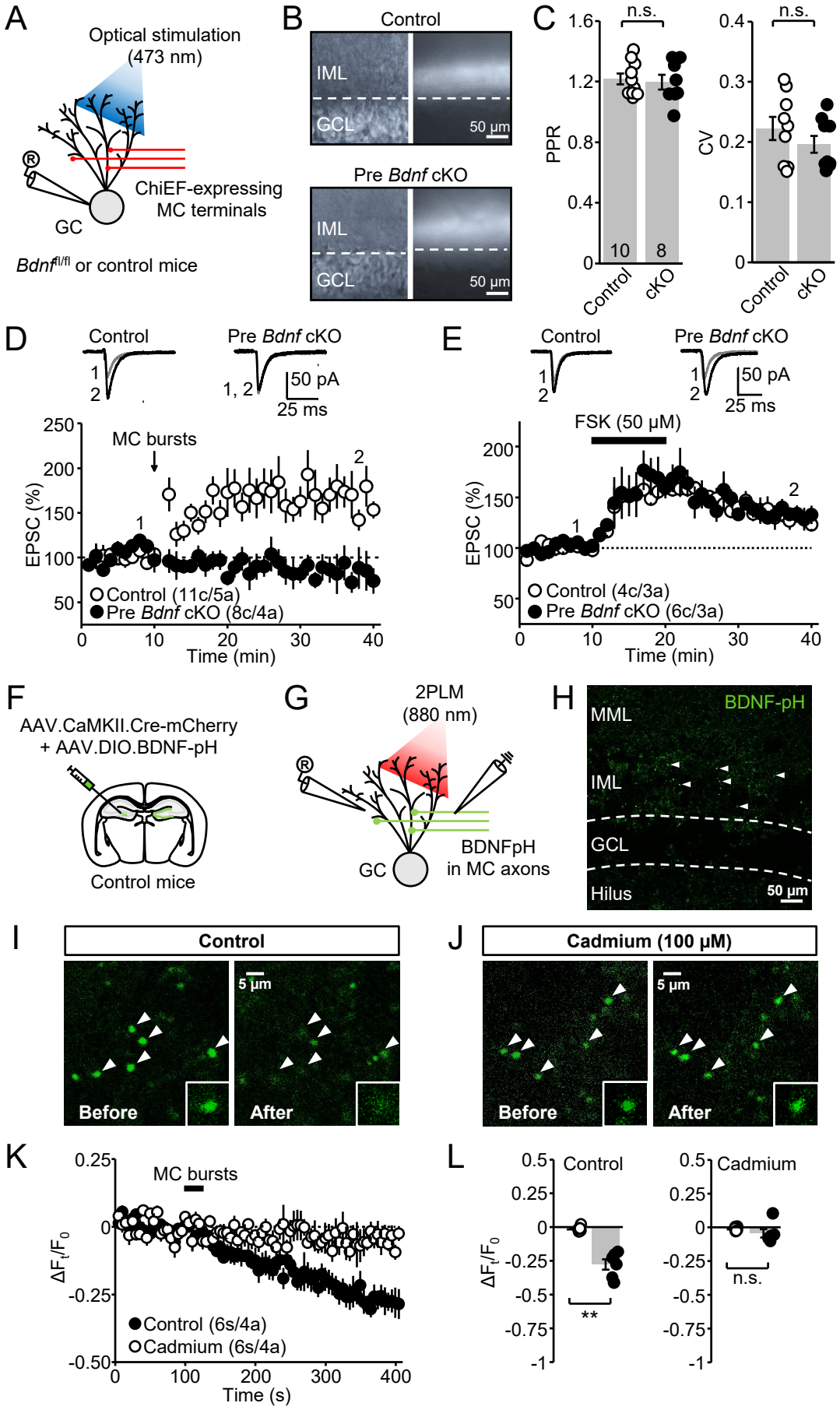

Figure 1. Presynaptic BDNF expression and release is required for MC-GC LTP

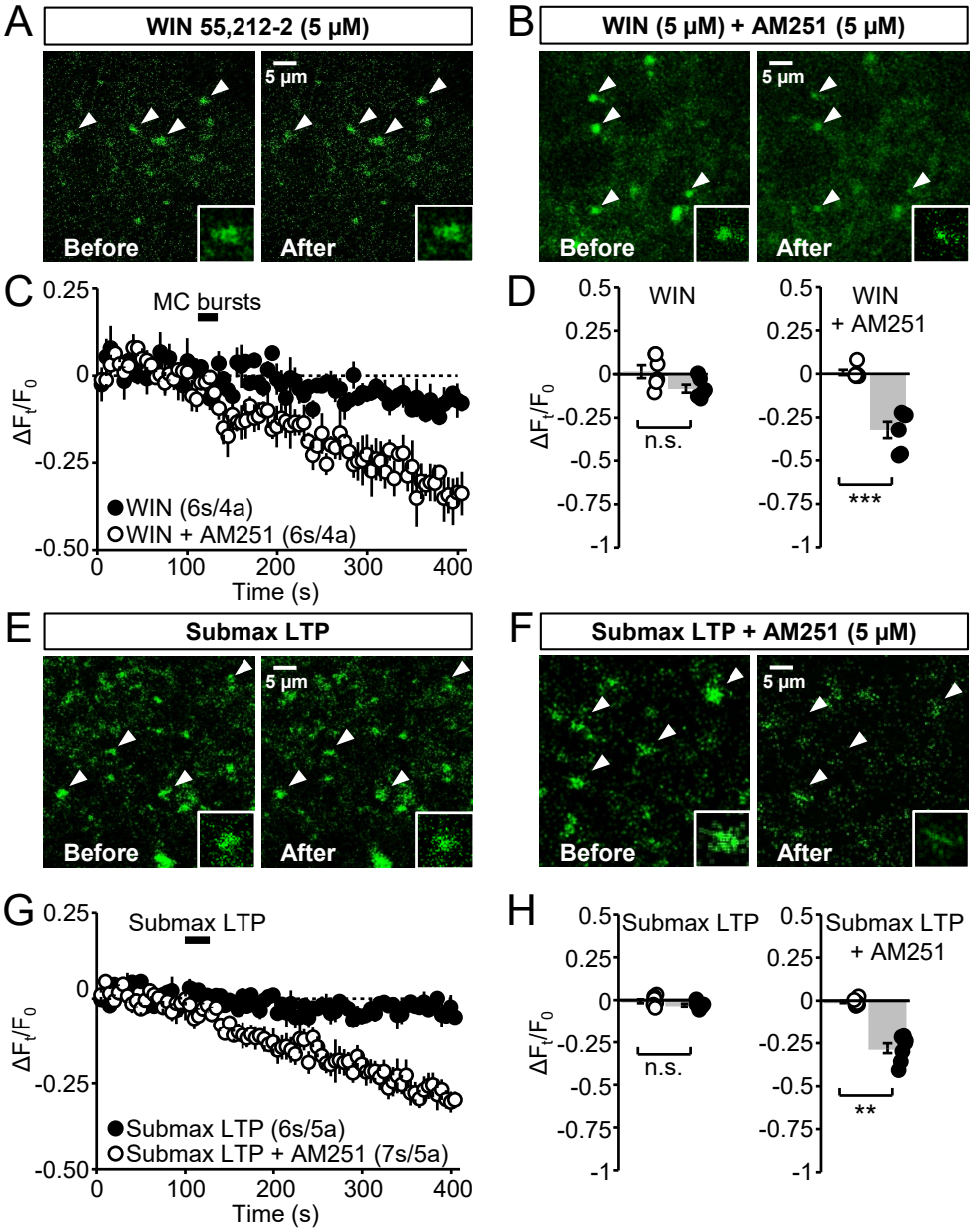

Figure 2. Presynaptic BDNF release is under the control of CB_1R activity

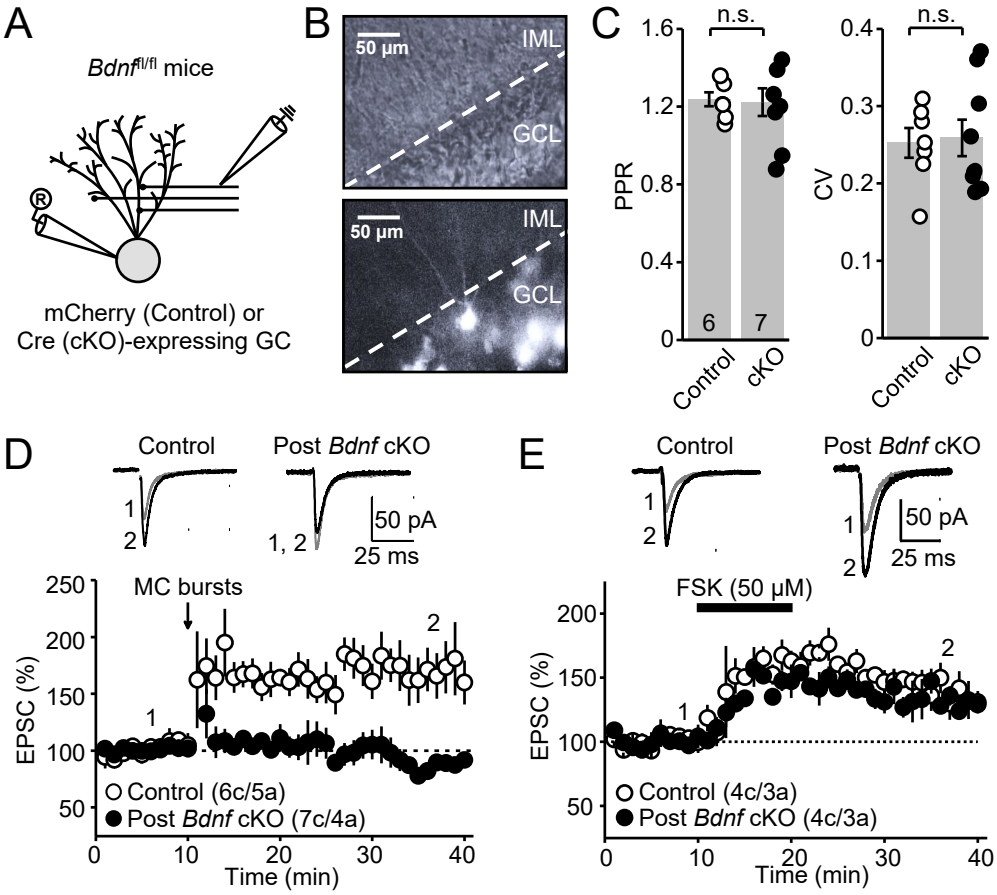

Figure 3. Postsynaptic BDNF is also required for MC-GC LTP

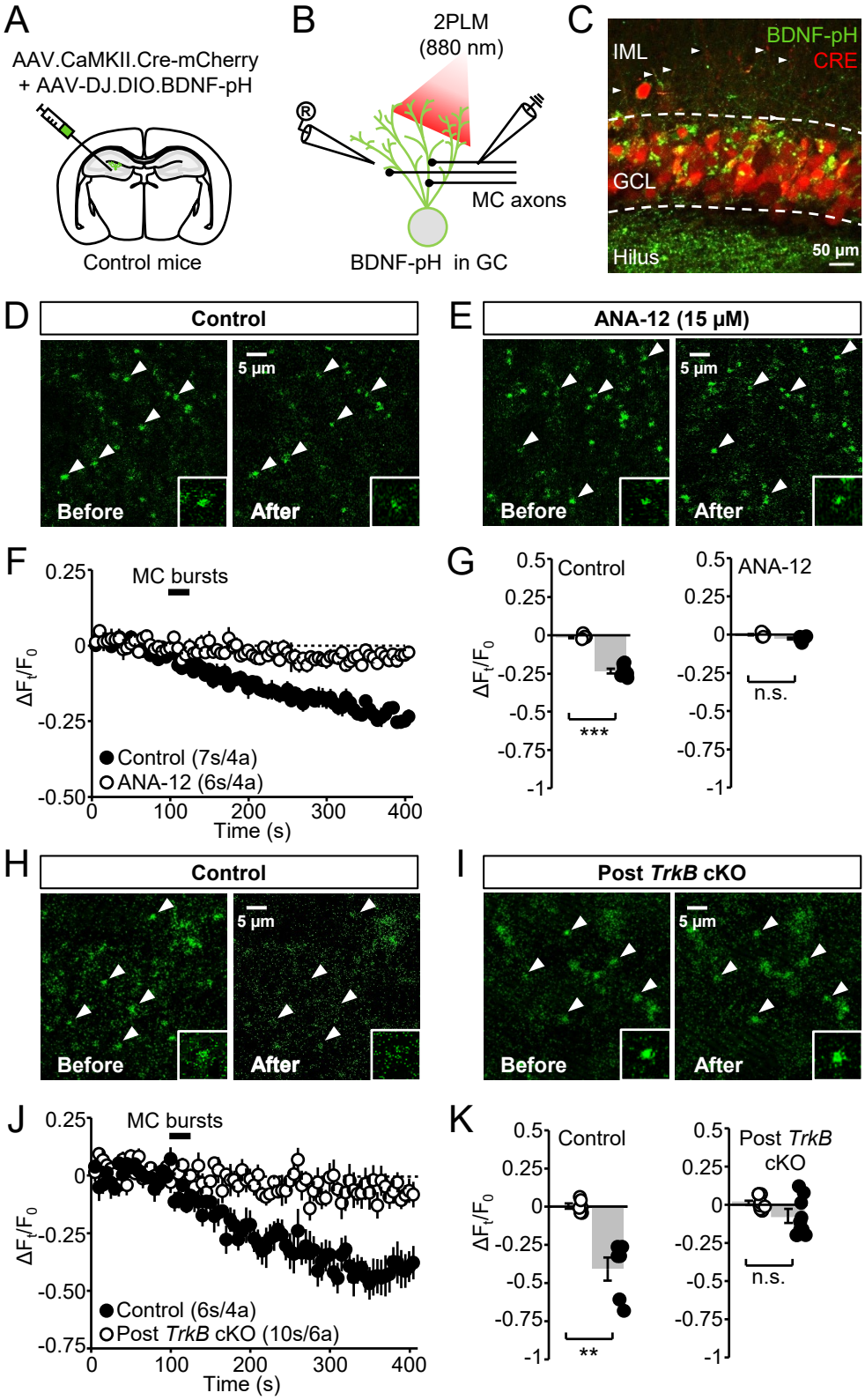

Figure 4. Postsynaptic BDNF release is TrkB-dependent

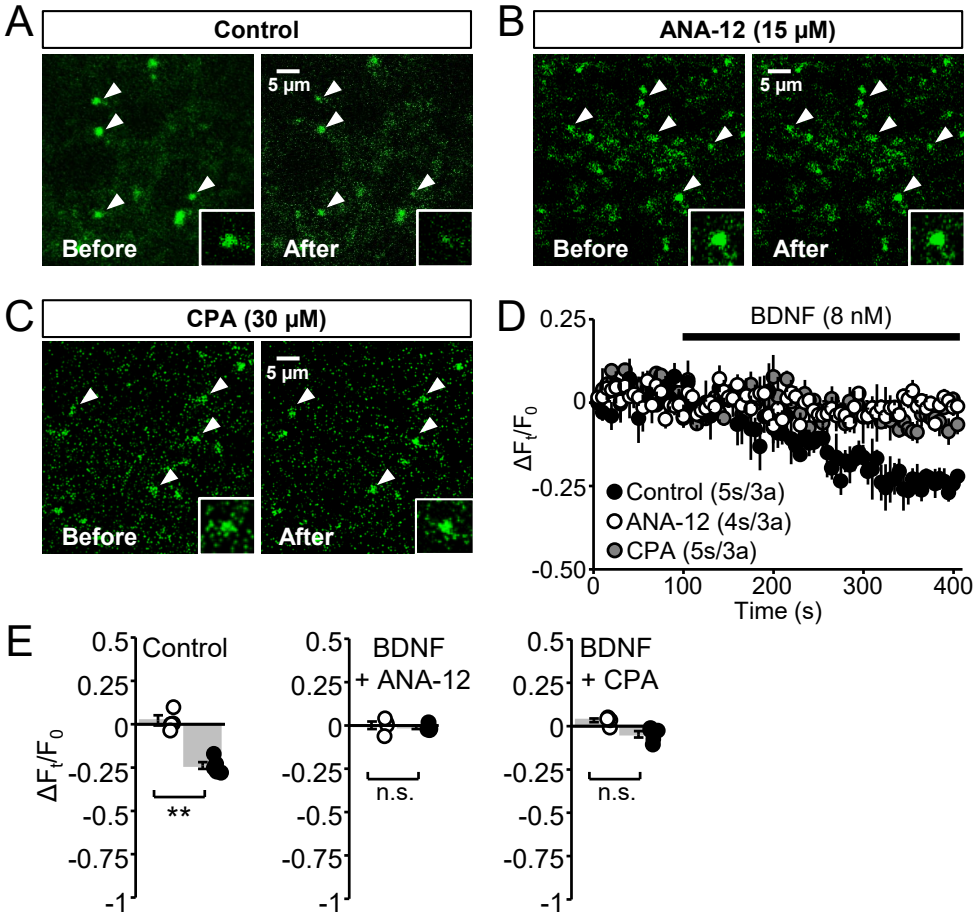

Figure 5. BDNF is sufficient to induce BDNF release by mobilizing calcium from internal stores

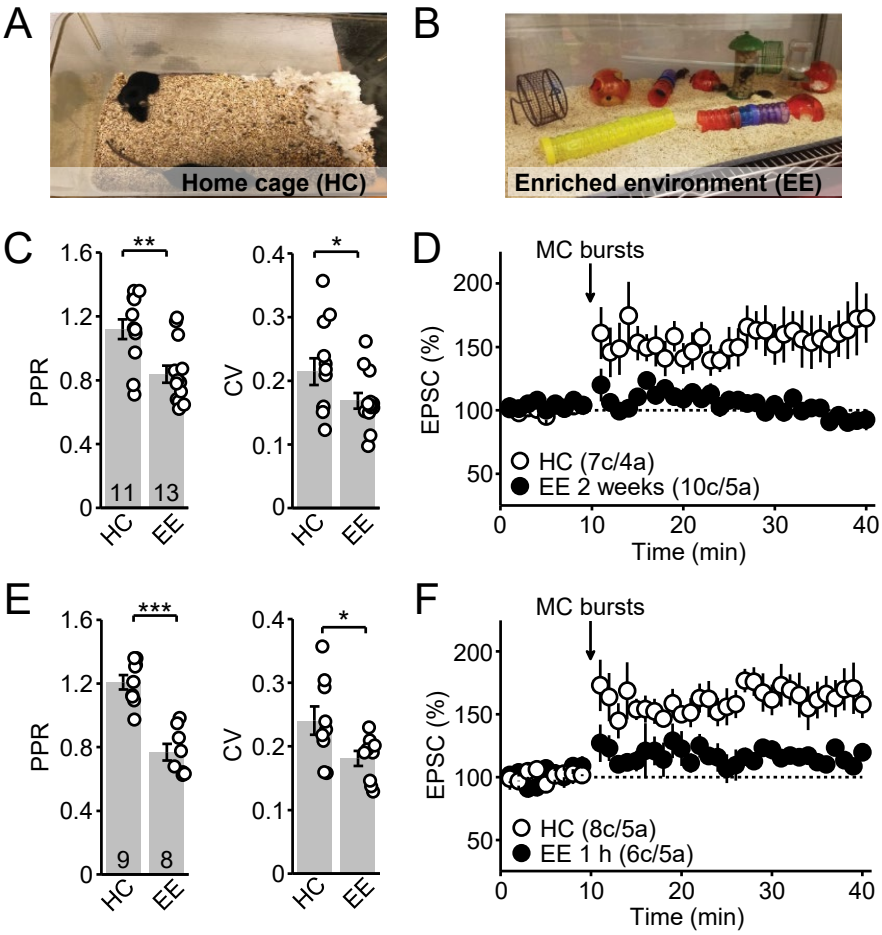

Figure 6. Exposure to enriched environment strengthens MC-GC synapses and occludes LTP

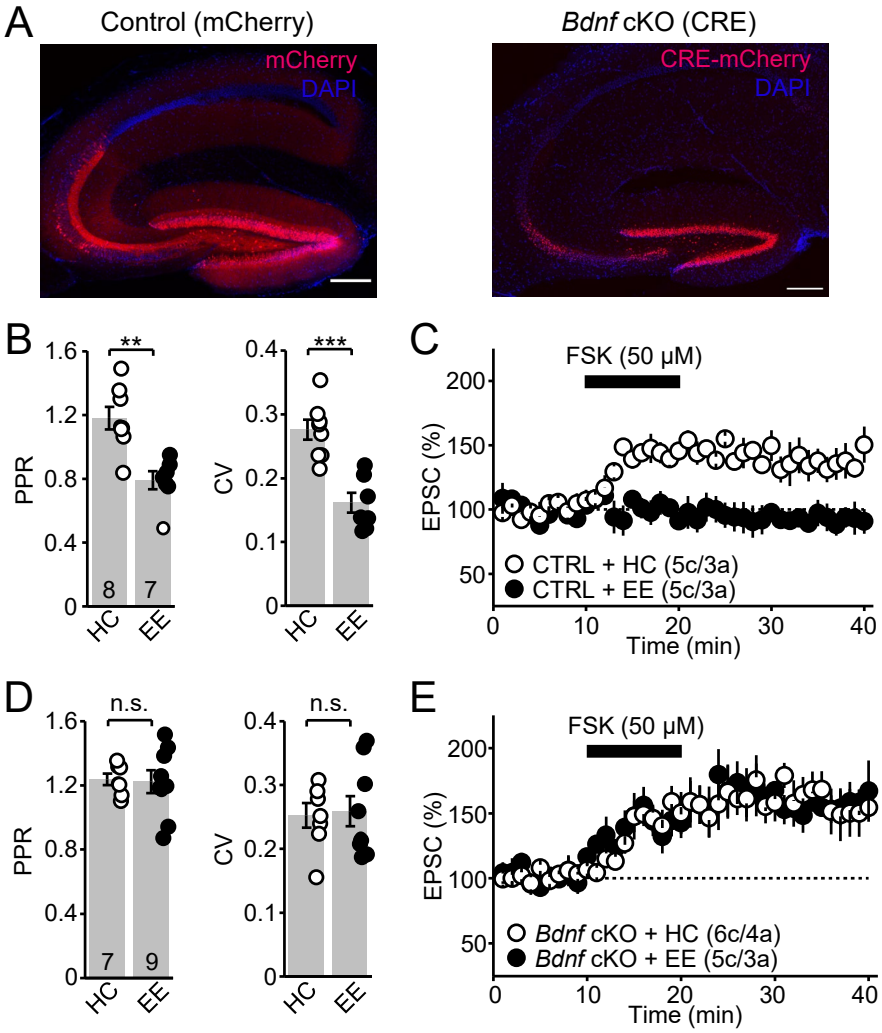

Figure 7. BDNF mediates activity-dependent LTP *in vivo*